Impact of trace metals Zn, Cu, Cd and Ni on the reactivity of OPC and GGBS-based hydraulic binders at early age for sediment stabilization

Tetiana Gutsalenko[1,2], Alexandra Bourdot[1], Valérie Montouillout[3], Aveline Darquennes[4], Thomas Wattez[2], Laurent Frouin[2], Mohend Chaouche[1]

[1] *Université Paris-Saclay, ENS Paris-Saclay, CNRS, LMT - Laboratoire de Mécanique et Technologie, 91190, Gif-sur-Yvette, France*
[2] *ECOCEM Materials, 4 place Louis Armand, 75012 Paris, France*
[3] *CEMHTI-CNRS UPR 3079, 1D avenue de la Recherche Scientifique, 45071, Orléans cedex, France*
[4] *Civil and Mechanical Engineering Laboratory, INSA de Rennes, 20 Avenue des Buttes de Coësmes, Rennes Cedex 7, France*

Abstract

The Solidification/Stabilization method was demonstrated to be an effective remediation technology for hazardous waste treatment. Three types of binding agents were tested in the present study in view of their potential use in solidification of contaminated sediments and soils – Portland cement (OPC), Granulated ground blast furnace slag (GGBS) activated by OPC and a Supersulfated (SSC) binders. An investigation into the impact of trace metals Zn, Cu, Ni and Cd on the hydration of the binders was performed by adding them into pure binders' systems. Hydration heat evolution of the binders was assessed through isothermal calorimetry and hydration products were analysed through XRD, NMR and XAFS analysis. Copper and zinc present the most perturbing effect on the early hydration delaying the main hydration peak occurrence while nickel and cadmium ions do not perturb or accelerate it. For example, the GGBS/OPC formulation without any metal addition has its MHP at 13.5h, with the addition of 0.5%Zn the MHP appears 37h later, with 0.5%Cu 11.5 h later, but with Ni and Cd 5 h earlier. The SSC formulation was shown to be the most sensitive on the trace metals addition. The electrokinetic and conductivity measurements of the binders using Zeta Potential apparatus showed a decrease in obtained values in the presence of Cu and Zn and an increase in the presence of Ni and Cd confirming the different behaviours of TM in the considered systems.

Keywords: solidification/stabilization| GGBS| trace metals| early age hydration| hydration kinetic|

1. Introduction

Different types of industrial wastes, sediments or soils are considered today as hazardous wastes because they contain a large amount of toxic trace metals (TM) that present a risk for natural ecosystem. For example, sediments are contaminated by pollutants from diverse industries located near ports, from stormwater runoff, effluents containing trace metals, pesticides, oils etc. In the marine environment, copper and zinc may occur from chemicals using for antifouling treatments [1,2]. Appropriate management of contaminated sediments/soils becomes a big challenge nowadays because of an increase of polluted sites. The Solidification/Stabilization (S/S) remediation strategy can be very effective in immobilization of inorganic contaminants [3]. Its importance has increased over last years due to the prosperous results of this cost-effective technology and increasing interest of researchers to use alternative cementitious materials [4–7]. Ground granulated blast furnace slag (GGBS) can be a good binder alternative to enhance mechanical and leaching performances of a polluted waste matrix [8–11]. Jin et al. [12] concluded in his study on soil stabilization that GGBS activated by MgO demonstrated increased strength and durability by decreasing the permeability of mixtures due to the denser microstructure of the slag-based samples. Generally, the stabilization of trace metals with hydraulic binders is achieved as a result of the formation of new insoluble precipitates or by the incorporation of trace metals ions into the hydration products developed through sorption or ion substitution processes [13]. However, these mechanisms may significantly vary depending on the type of binder, its pH, redox potential, hydration kinetic, types of precipitated hydrates [14,15].

The Stabilization/Solidification process may depend on the different constituents of the treated waste, which often presents as a heterogeneous system [16]. During the treatment of industrial residues or sediments/soils, retardation or even inhibition of cement set may occur affecting desired properties of a final material [17]. The type of trace metals, their ionic radii and concentration may impact in a different way the hydration kinetic of binders and the growth and nucleation of hydrates [18].

Numerous studies have attempted to explain the mechanisms involved in the retardation/acceleration of cement systems [19–22]. Some trace metals are thought to cover cements' grains like a protective membrane of amorphous hydroxides species and preventing further dissolution of binders [23]. However, there is a lack of direct evidence of such mechanism and the experimental data are rather controversial. Scrivener et al. [24], Weeks et al. [25] make doubt about the protective membrane

theory because such membrane has never been detected even with help of advanced modern tools. Another possible retardation mechanism can potentially arise from the delayed nucleation of some important hydrates giving the early hydration and providing hardening of the treated material [26]. This theory explains the induction period by the slow nucleation and growth of hydrates such as portlandite (CH) and calcium silicate hydrates (C-S-H) until the supersaturation of the solution [27,28]. In addition, some theories explain the induction and acceleration period only by the C-S-H nucleation and growth which starts from the very beginning of hydration [29]. The recent theory of undersaturation of solution and dissolution of minerals is proposed in the literature. The theory explains a non-linear decrease in dissolution rate of minerals with the undersaturation decrease, meaning that the system goes towards equilibrium [24]. With the decrease in degree of undersaturation of solution the reactions' rate decrease severely and is related to the induction period on calorimetry curves. With the increase of degree of undersaturation in the end of dormant period, the cement dissolution takes place [29,30]. After supersaturation with high enough concentration of calcium and silicates in solution, the massive nucleation of stable C-S-H occurs [31]. However, further works need to be done in order to validate the theories and explain the first hydration steps of complex cement systems, especially with orientation to the alternative cementitious materials and their use for the waste treatment. The complexity arises from the variation of each type of a binder as well as from the coupling processes of dissolution-growth of hydrates. In a general sense, the extended induction period of the cements systems in presence of foreign ions such trace metals may have two origins: ion-ion interaction or interactions taking place at the surface of a solid in a solution [32,33].

There are relatively few studies on the mechanisms changing the hydration kinetic of GGBS-based binders in presence of trace metals [34–36]. Yoon et al. [35] reported an acceleration effect of cobalt through the rapid precipitation of Afm and LDH phases in the Portland cement/Blast furnace slag samples. However, the retardation effect occurs after the addition of lead to the OPC/GGBS mixtures in the study of Hekal et al. [34]. Garg and White [36] investigated the mechanisms of zinc oxide retardation in alkali-activated GGBS. Regrading some other binders, in the work of Niu et al. [37] the impact of Cr^{3+}, Pb^{2+}, and Cd^{2+} heavy metls in form of nitrate salts on the hardening of CSA and OPC were investigated. An important delay in hydration was observed almost for all stuidied samples

through measuring setting time, but little effect on compressive strength. In the study of Keppert et al. [38] it was shown that the initial setting time of the cement mixed with contaminated ceramic waste was considerably impacted by the presence of Cu, Zn and Pb – the hydration was retarded except zinc with lower dosages of ceramic waste. The compressive strength was also negatively impacted, especially in the case of Cu. Li et al. [39] studied the potential immobilization of Cu^{2+} and Cr^{3+} in LDH-type phase hydrotalcite as a common hydration products in OPC containing GGBS. It was shown that both heavy metals are well immobilized in LDH through isomorphic substitution for Mg^{2+} or Al^{3+} using slags rich in magnesium.

The present study was designed to determine the effect of Zn, Cu, Ni, Cd trace metals on the early hydration of Supersulfated and GGBS-rich binders in comparison with plain OPC binder, in order to optimize the S/S process and enhance its efficiency in various applications, e.g. in road industry, in construction of base and fondation layers, as aggregates, as a material for bricks production . The compressive strength results of the study [40] showed that the Supersulfated formulation did not get a sufficient strength to be measured after being mixed with the contaminated sediment. The GGBS-rich mix demonstrated the lower strength at 28 days compared to the OPC mixture, however at long term storage the strength of the samples with GGBS exceeds that of cement-based mixes. These findings demonstrate quite different kinetic of hydration of different types of binding agents once mixed with contaminated sediments, which can potentially result from the interaction with trace elements. Therefore, we proposed model systems based on the studied binders and four types of metal cations introduced separately into the binders. The metal cations are Zn, Cu, Ni and Cd, in the form of nitrate salts, chosen according to their abundance in polluted soils/sediments matrix as well as to the difference in their ionic size. This approach was largely applied in the field of cementitious materials interacting with heavy metals [21,37,38,41,42], however there is a little published data on the impact of these metals on the hydration of GGBS-based binders.

The aim is to understand how each of these trace metals interacts with the blast furnace slag binders in comparison to the widely used OPC cement for stabilization/solidification, the mechanisms responsible for the early hydration of GGBS-based binders and what products would potentially be

formed. To address this objective, the study focuses on monitoring hydration at early age by isothermal calorimetry and XRD to characterise the impact of the selected trace metals on the hydration kinetic of the binders. Then, the surface charge of the binders, that can be impacted by the size and type of an ion as well as by the ionic strength of the solution [40], was monitored by measuring the zeta potential. Finally, the element specific advanced analytic tools, nuclear magnetic resonance (NMR) spectroscopy and XAFS, are used to determine the products formed and their potential effect on the hydration products.

2. Materials

2.1. Binders

The Ordinary Portland cement was supplied by Vicat Cement group which is located in Fos-sur-mer, France. The ground granulated blast furnace slag was provided by ECOCEM France factory also situated in Fos-sur-Mer. The GGBS was manufactured according to NF EN 15167-1 [43] with the Blaine fineness of 4500 cm²/g. The chemical composition of both hydraulic binders is presented in Table 1. The chemical analysis was performed using X-Ray Fluorescence (Philips PW 1404 X spectrophotometer) with high reproducibility linked to industrial quality control. For the preparation of the Supersulfated formulation (SSC) the anhydrous calcium sulfate $CaSO_4$ (99% of purity from Alfa Aesar) was used.

Binder	**Oxide (Dry, wt.%)**									
	CaO	SiO_2	Al_2O_3	Fe_2O_3	TiO_2	MgO	Na_2O	K_2O	SO_3	LOI
GGBS	43.9	37.6	10.26	0.33	0.81	6.93	0.22	0.26	0.03	-
OPC	64.06	20.01	3.96	3.08	0.17	1.25	0.15	0.74	5.20	1.26

Table 1 Chemical composition of GGBS and OPC

2.2. Mix design ‘Binders-TM’

In order to investigate the impact of trace metals on the hydration of the considered binders, the hydrated nitrate salts were ordered from Sigma Aldrich such as Cadmium nitrate tetrahydrate $Cd(NO_3)_2.4H_2O$, Nickel nitrate hexahydrate $Ni(NO_3)_2.6H_2O$, Copper nitrate trihydrate $Cu(NO_3)_2.3H_2O$ and Zinc nitrate hexahydrate $Zn(NO_3)_2.6H_2O$. Nitrates salts were chosen due to their high solubility. It is known that calcium-nitrates may accelerate cement hydration via the formation of Afm through the

145 reaction of C3A and NO_3^- [44]. In the work of Matejka et al. [45] different Zn salts ($ZnCl_2$, $Zn(NO_3)_2$,
146 ZnO) were mixed with ordinary Portland cement – in all the cases the hydration was retarded with
147 nitarets and chlorides having less induction period compared to zinc oxides.
148 The binders made of plain OPC, GGBS-rich mix and Supersulfated cement, respectively noted OPC,
149 GGBS85 and SSC, were mixed with trace metals solutions (Table 2), the samples are designated as
150 (wt.% of a trace metal)(Trace metal)(Binder) in the present study. The nitrate salts were dissolved in
151 demineralized water and then used as a mixing water for the samples preparation with the water:binder
152 ratio of 0.4. The range of trace metals added in this study corresponds to the amount of trace metals
153 contained in contaminated sediments considered in [40] and these concentrations are typical for
154 industrial soils[46,47]. The remaining paste was put in small plastic tubes and protected with parafilm
155 to avoid carbonation. The samples for the XRD, NMR and XAFS analysis were grinded in a mortar
156 and pestle and soaked in isopropanol before being dried in air-circulating oven for 24 hours at 40°C
157 after the proper curing duration (7 days, 28 days and 3 months depending on the analysis method).

Samples	**Trace metals salts (wt% binder)**			
	$Zn(NO_3)_2$	$Cu(NO_3)_2$	$Cd(NO_3)_2$	$Ni(NO_3)_2$
OPC (100%Portland cement)	0%; 0.1%; 0.5%; 2%			
GGBS85 (85%GGBS/15%OPC)				
SSC (85%GGBS/14%$CaSO_4$/1%OPC)				

158 Table 2 Mix design of the hydraulic binders with trace metals in form of nitrate salts
159

160 **3. Methods**

161 3.1. Isothermal calorimetry

162 The Tam Air isothermal calorimeter from TA Instruments was used to evaluate the heat release of the
163 specimens over 72 h of hydration with thermostat set at 22°C. The reference cell contained the blank
164 sample of 5g of silica sand and 2.5g of tap water. The dry binders were put in contact with water or
165 TM solution and mixed during 1 min before being introduced into the calorimeter cells at 5g per cell.
166 The cumulative heat release during 72 h of hydration was calculated without taking into account the
167 first hour of measurements to avoid the imbalance of the system due to the cell opening to put the
168 sample.
169

3.2. XRD analysis

The hydration of the binders mixed with TM nitrate salts was stopped after 24 hours and 7 days of storage and the samples were ground with mortar and pestle for X-ray diffraction. The measurements were done using the apparatus D2 PHASER from BRUKER with the anode in cobalt as metal target (λ=1.79Å) and with the step size of 0.02° and 1.2s counting time per step. Only crystalline phases were analysed due to the complexity of amorphous phases assemblage.

3.3. Zeta Potential measurements

Zeta potential measurements were carried out using the Zetaprobe Analyser from Colloidal Dynamics performing through the electroacoustic method. The electrokinetic properties of the OPC-based binder (OPC) and GGBS-based binder (GGBS85) in the presence of 0.5% of trace metals salts were measured. For this purpose, the powder of each type of binders was put in a trace metal solution in ratio 50 g/L with permanent stirring at 250 rpm. The values of Zeta potential and conductivity were recorded every 2 minutes for 1 hour.

3.4. NMR investigation

The local environment of aluminium in the OPC and GGBS85 binders' systems with and without zinc and cadmium nitrate salts addition was probed by solid state NMR in the CEMHTI laboratory (Orleans, France). The study of Cu and Ni systems was made dubious due to the paramagnetic properties of these isotopes. ^{27}Al spectra were recorded at room temperature using a Bruker AVANCE 850MHz spectrometer (20 T magnetic field) operating at 221.6 MHz for ^{27}Al. The MAS spinning speed was fixed at 30 kHz and the spectra were acquired after a 0.5µs short pulse (flip angle π/18) ensuring quantitative reliability of the intensities. Around 36000 scans were accumulated with 1s relaxation delay. ^{27}Al chemical shift were referenced to 1M aqueous solution of $Al(NO_3)_3$. ^{29}Si MAS and $\{^1H\}$-^{29}Si CP-MAS spectra were acquired on a Bruker AVANCE III 400 MHz (9.4 T magnetic field) spectrometer operating at 400 and 79.4 MHz for ^{1}H and ^{29}Si respectively. The MAS spinning rate was fixed at 8kHz using a 7mm probehead. The MAS spectra were acquired after applying a 5µs pulse (flip angle π/4). Around 5000 scans were accumulated with a 10s recycling delay. CP-MAS

198 spectra were acquired using a 5ms contact time, around 50000 scans were added using a 1s recycling
199 delay. Tetramethyl silane (TMS) was used as reference compound for ^{29}Si. All the spectra were
200 simulated using the DMFit software [48].
201
202 3.5. XAFS investigation
203 XAFS experiments were carried out for the OPC and Supersulfated mixes doped with 0.5% of $CdCl_2$
204 after 28 days of storage. They are conducted at the Argonne national laboratory at the 5-BMD
205 beamline. Only the x-ray absorption measurements have been studied. All intensity spectrums are
206 recorded around Cadmium K-edge (26.711 keV) from 26.500 keV to 27.300 keV. Due to the lack of
207 pure cadmium to calibrate the measure, calibration was performed with CdO and CdCl samples.
208 EXAFS data analysis was performed using the ATHENA/ARTEMIS software. The software does
209 automatically background reduction and normalization of the spectra. The X-ray absorption near edge
210 structure gives information on the local coordination environment and the element oxidation state.
211 This technique allows determining the speciation of cadmium in samples. The radial structure function
212 is obtained by Fourier transformation of the k^3-weighted $c(k)$ function between 0.3 nm^{-1} and 1
213 nm^{-1} Then an identification analysis is carried out to obtain information about the phases formed
214 during the samples hydration. A linear combination fit (Eq.1) is made from compared pure phases c
215 function to samples between 0.1 and 0.8 nm^{-1}. Above 0.8 nm^{-1} the signal is too noisy to be
216 interpreted. The criterion used to determine the best combination is the minimum of the R-factor.
217 $\chi_{mixture} = \sum_{i=1}^{n} f_i \chi_i$ (Eq. 1)
218
219 **4. Results**
220 4.1. Hydration heat – calorimetry measurements
221 The results of the heat evolution of three types of binders OPC, GGBS85 and SSC mixed with various
222 dosages of trace metals nitrate salts are summarised in Table 3. The plain OPC binder once mixed
223 with different amounts of zinc nitrate salt exhibits changes in the hydration behaviour (Fig. 1, (a)). For
224 the control mixture the main hydration peak (MHP), corresponding to the rapid growth of CH

225 (portlandite) and C-S-H, occurs at 11.4 h with the endothermic reaction of 3.87 mW/g. At the small
226 dosage of 0.1%wt zinc leads to the acceleration of hydration kinetic with MHP occurring at 8.7 h and
227 with slightly higher heat rate release. However, a delay in hydration can be observed for higher
228 dosages of zinc. The induction period is longer with MHP appearing at 13.6 h and 19.4 h, with more
229 important heat rate of 4.8 mW/g and 6 mW/g when $Zn(NO_3)_2$ dosage were respectively set at 0.5%wt
230 and 2%wt. The value of the total heat flow after 72 h of hydration progressively decreased with
231 increasing zinc dosage. In a study investigating the impact of zinc on cement hydration, Keppert et al.
232 [38] demonstrated that Zn caused hydration delay with a significant extension of induction period,
233 especially with the highest dosage of zinc. Matejka et al. [45] also showed an important retardation of
234 hydration of plain OPC formulation doped with $ZnCl_2$, $Zn(NO_3)_2$ or ZnO at different dosages (0.1%,
235 0.5% & 1%) via calorimetry test.
236 The introduction of copper nitrate into the OPC binder changes considerably the early hydration
237 except the smallest dosage. The addition of 0.1% of $Cu(NO_3)_2$ only slightly changed the OPC
238 hydration kinetic with MHP occurring 1 h later. As can be seen in Table 3, the 0.5% dosage of
239 $Cu(NO_3)_2$ shortened the induction period with MHP at 9.3 h. Nevertheless, the mixture with 2% of
240 copper salt exhibits an important retardation effect with the total heat flow considerably lower than the
241 one determined for the control sample. For the cadmium doped OPC mixtures, there is a tendency of
242 accelerated hydration for all dosages. With the increase of the cadmium salt dosage, the acceleration
243 effect becomes more noticeable. However, the heat release decreases to some extent gradually with the
244 increase of the cadmium nitrate amount. The introduction of nickel nitrate at different dosages into the
245 OPC formulation presents almost the same tendency as cadmium nitrate – the hydration reactions
246 were accelerated and the induction period was considerably shortened, especially for the 2%NiOPC
247 mixture. The 0.1% $Ni(NO_3)_2$ and 0.5% $Ni(NO_3)_2$ dosages show almost the same hydration behaviour
248 with earlier occurrence of MHP at 7-8 h almost without changing the heat rate release of the MHP of
249 the control mixture.

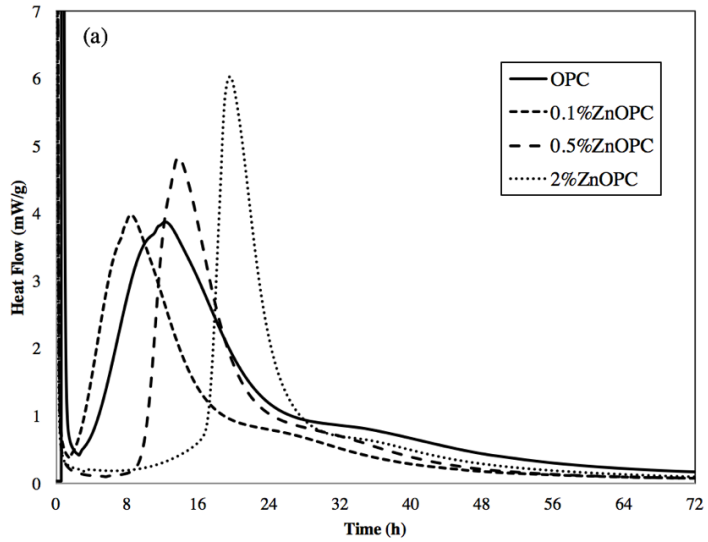

250

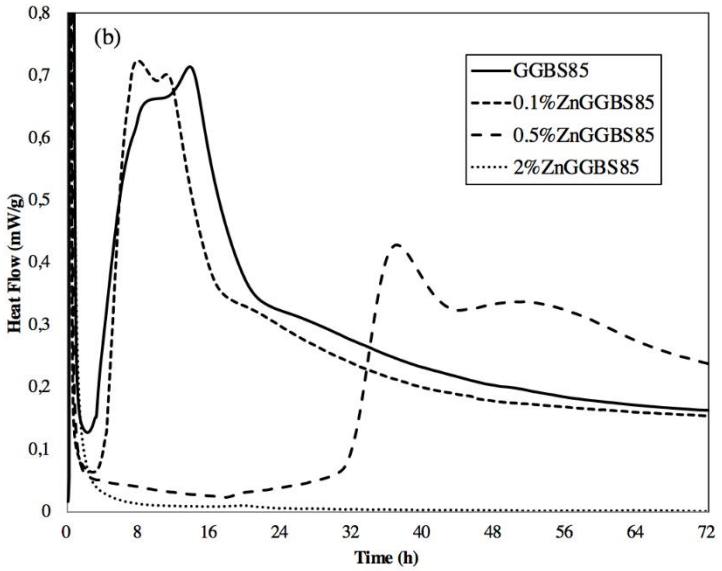

251

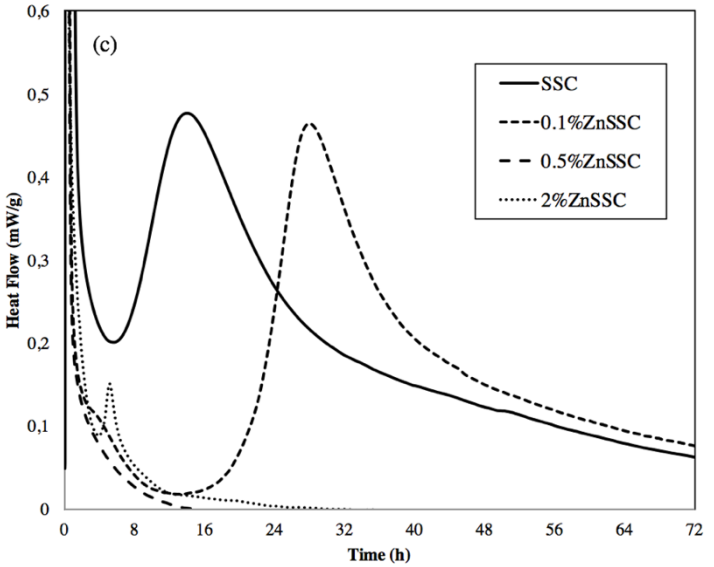

252

253 Fig. 1 Hydration heat evolution of OPC (a), GGBS85 (b) and SSC (c) mixed with zinc nitrate at
254 0.1%wt, 0.5%wt and 2%wt

		OPC				GGBS85				SSC			
	Dosage	*0.0%*	*0.1%*	*0.5%*	*2.0%*	*0.0%*	*0.1%*	*0.5%*	*2.0%*	*0.0%*	*0.1%*	*0.5%*	*2.0%*
$Zn(NO_3)_2$	Main hydration peak (h)	11.4	8.7	13.6	19.4	13.5	10.9	50.7	-	14.0	28.3	-	-
	Peak height (mW/g)	3.87	3.96	4.80	6.00	0.71	0.70	0.34	-	0.48	0.46	-	-
	Total Heat Flow 72h (J/g)	274.8	205.6	201.7	192.9	76.7	68.5	50	2	50.9	39.4	2.3	4.2
$Cu(NO_3)_2$	Main hydration peak (h)	11.4	12.4	9.3	37.9	13.5	15.4	25.0	-	14.0	41.3	-	-
	Peak height (mW/g)	3.87	3.85	3.79	2.44	0.71	0.70	0.08	-	0.48	0.41	-	-
	Total Heat Flow 72h (J/g)	274.8	267	205.5	163.1	76.7	72.3	12	3.1	50.9	39.8	18.3	1.6
$Cd(NO_3)_2$	Main hydration peak (h)	11.4	7.7	6.4	4.0	13.5	10.2	8.2	18.8	14.0	13.5	19.6	32.9
	Peak height (mW/g)	3.87	3.89	3.59	3.20	0.71	0.61	0.60	0.35	0.48	0.52	0.42	0.32
	Total Heat Flow 72h (J/g)	274.8	192.5	180.9	151.5	76.7	71.1	67.7	60.8	50.9	41.4	38.4	33.8
$Ni(NO_3)_2$	Main hydration peak (h)	11.4	7.9	7.6	6.0	13.5	8.8	8.2	8.6	14.0	11.4	8.8	32.9
	Peak height (mW/g)	3.87	3.88	3.80	3.60	0.71	0.70	0.69	0.71	0.48	0.47	0.24	0.25
	Total Heat Flow 72h (J/g)	274.8	208.6	196.1	186.2	76.7	64	58.3	78.1	50.9	37.5	40.3	41.5

Table 3. Hydration heat rate results of OPC, GGBS85 and SSC mixed with Zn, Cu, Cd, Ni in the form of nitrate salts

The hydration of the GGBS85 formulation doped with trace metals varies considerably according to their concentration and the type of metal. The main hydration peak of the control mixture of GGBS85 is referred to the pozzolanic reaction of GGBS following the Portland cement hydration using as an activator of the system. It occurs at 13.5 h after mixing with water releasing 0.71 mW/g of heat. 0.1%ZnGGBS85 exhibits an acceleration of the occurrence of the main peak of hydration (Fig. 1, (b)). Meanwhile, the higher zinc dosages significantly impacted the early hydration of the formulation. The 0.5%$Zn(NO_3)_2$ dosage has an important retarding effect with MHP occurring at 50.7 h with two times lower heat release of 0.34 mW/g and with acceleration period that starts and ends at longer time. Moreover, the introduction of 2%$Zn(NO_3)_2$ into the GGBS85 mixture completely annihilated the early hydration process. The induction period of 0.1%CuGGBS85 was extended with the main hydration peak of acceleration-deceleration stages occurring at 15.4 h, but almost without changing the hydration evolution compared to the control mixture. However, the higher dosages of Cu^{2+} had a severe negative impact on the early hydration of GGBS85. 2%CuGGBS85 was impacted in the same way as 2%ZnGGBS85 with a complete annihilation of the hydrates formation. Cadmium nitrate at 0.1% and 0.5% dosages once mixed with GGBS85 shortened the induction period. At the same time, the heat rate corresponding to the pozzolanic reaction of GGBS was lower for both dosages ~ 0.6 mW/g, but the pre-peak of the acceleration stage relating to the Portland cement hydration remained higher than in the control sample producing stronger endothermic reactions. The introduction of 2%

277 $Cd(NO_3)_2$ retarded the hydration of the mixture with the MHP occurring at 18.8 h and producing half
278 the heat of the control mixture with acceleration period starting and ending at longer time. However,
279 this retardation effect is much less severe compared to the effect of copper and zinc. With respect to
280 GGBS85 mixed with nickel nitrate salt, the general tendency demonstrates the acceleration of the
281 hydration reactions for the all considered dosages of Ni^{2+}. The heat rate released for the MHP of all
282 mixtures has almost the same value as the reference formulation, however the cumulative heat
283 produced over 72 h of measurements was slightly lower for 0.1%NiGGBS85 and 0.5%NiGGBS85,
284 but higher for 2%NiGGBS85.
285 The Supersulfated (SSC) formulation seems to be the most negatively impacted by the addition of zinc
286 nitrate salt compared to OPC and GGBS85 (Fig. 1, (c)). The main hydration peak of the control
287 sample of SSC was recorded after 14 h of hydration with the heat rate release of 0.48 mW/g. In the
288 presence of 0.1% of $Zn(NO_3)_2$ the induction period of SSC was twice as long. The MHP was
289 considerably delayed occurring only after 28.3 h but with almost similar heat rate. At the higher zinc
290 dosages of 0.5%wt and 2%wt no hydration reactions were detected over entire period of the
291 calorimetry measurements. The impact of copper on the hydration of the Supersulfated formulation is
292 even more noticeable. This time the MHP for 0.1%CuSSC occurred only after 41.3 h but the heat rate
293 of the endothermic reactions corresponding to the MHP was not as strongly affected. The reactivity of
294 the Supersulfated binder was completely annihilated in the presence of higher copper dosages. The
295 introduction of cadmium nitrate salt into the SSC formulation had the least negative impact on
296 hydration over 72 h of the calorimetry measurements. For the 0.1%CdSSC mixture the MHP occurs
297 after 13.5 h meaning the slight acceleration of hydration with higher heat rate of 0.52 mW/g. With
298 further progressive increase in the content of cadmium nitrate, the occurrence of the main peak of SSC
299 was retarded, but not completely annihilated as in the presence of copper or zinc. The addition of
300 0.1%$Ni(NO_3)_2$ shortened the induction period even more than 0.1%$Cd(NO_3)_2$ with the MHP occurring
301 after 11.4 h without impacting the heat rate release. The 0.5%NiSSC formulation also demonstrated an
302 acceleration of the main reactions of hydration, however the measured heat rate of MHP value was
303 two times lower than in the case of the control formulation. The addition of 2% $Ni(NO_3)_2$ produced the
304 same extension of the induction period as 2%wt of cadmium with the occurrence of the MHP after

32.9 h, nevertheless the measured heat rate of the MHP (0.25 mW/g) was lower than for cadmium nitrate.

4.2. XRD analysis

Main hydration products of the binders were identified via XRD technique (Fig. 2). Almost no difference in the hydration products development can be observed for the control OPC formulation and with addition of 0.1% and 0.5% of $Zn(NO_3)_2$ (Annex). At the same time for the dosage of 2% of zinc nitrate there is a higher amount of calcite and lower amount of portlandite precipitation at 24 h (Fig. 2, (a))). The calcite amount can refer to the carbonation of the sample due to the effect of zinc during the deceleration and hardening period (8-24 h) previously reported by Chen et al. [13]. This phenomenon was also observed by McWhinney and Cocke [49] and explained by lowering of the buffering capacity of calcium due to the presence of different metal cations. The suppression of Portlandite with Zn addition into OPC was reported in the study of Keppert et al. [38].

The most remarkable effect of the copper nitrate solution was obtained at 2%$Cu(NO_3)_2$ dosage – as can be seen on the graph the anhydrous peaks of C_2S and C_3S seem to be unreacted at 24 h. The portlandite phase was not formed and the ettringite peak is the only hydration product present in important amount for 2%CuOPC mixture at 24 h. The intensity of the calcite peak is higher for 2%CuOPC compared to the other samples, it can be related to accelerated carbonation.

There was no significant difference in hydrates formation for the control sample and the samples containing nickel, except for the higher dissolution rate of C_2S and C_3S with 0.5%$Ni(NO_3)_2$. The lowest amount of portlandite was precipitated in the case of 2%NiOPC as well as the highest amount of calcite. At the first glance it seems that the ettringite phase is more abundant for 2%$Ni(NO_3)_2$. It can be supposed that nickel promoted the formation of ettringite and therefore the acceleration observed in calorimetry. The X-ray diffractograms of the OPC formulation mixed with cadmium nitrate at different dosages show a uniform evolution of the hydration products after 24 hours, as well as after 7 days of storage.

On the other hand, almost no difference in hydration products formation was noticed after 7 days of storage for the control sample and for OPC doped with TM (Annex). The only difference that stands out on the graph is the slightly higher dissolution rate of C_2S, C_3S for 0.5%NiOPC and an increase in ettringite intensity for the 2%CdOPC mixture at 7 days.

In the case of GGBS85 there are more visible modifications of the hydration reaction depending on the type of metal at the considered hydration period. The XRD analysis after 24 hours of hydration of GGBS85 shows the precipitation of ettringite and portlandite (Fig. 2, (b)). With the introduction of 0.1%$Zn(NO_3)_2$, the intensity of these hydrates was two times lower. However, in the case of 0.5% and 2% zinc nitrate addition, only the ettringite phase was formed. The absence of portlandite goes in accordance with the presence of anhydrous peaks of C_2S, C_3S compared to their important dissolution rate in the case of the reference GGBS85 formulation as well as for 0.1%ZnGGBS85. The dissolution of anhydrous phases C_2S and C_3S was also inhibited by the introduction of 0.5% and 2% of copper salt. At the same time the ettringite phase is present at all dosages of copper nitrate at 24 h. The evolution of the hydration products of the GGBS85 sample and 0.1%NiGGBS85 is pretty similar after 24 h. By increasing the amount of nickel salt to 0.5%$Ni(NO_3)_2$, there is significantly less precipitated portlandite. In the presence of 2% $Ni(NO_3)_2$, the dissolution of C_2S, C_3S was inhibited, consequently no portlandite phase can be detected after 24 h. However, the highest intensity of the ettringite peak was obtained for 2%NiGGBS85 as in the case of the OPC formulation. After 24 h of hydration, all samples of the GGBS85 formulation with cadmium addition show the precipitation of portlandite, ettringite and calcite. The ettringite phase was precipitated in almost equal amount for all samples but not portlandite. The lowest intensity of portlandite peak was attributed to 0.1%CdGGBS85 and the highest peak to 0.5%CdGGBS85.

After 7 days of storage the formation of C-S-H was annihilated with increase in TM amount, especially from 0.5%wt dosage for Cu and from 2%wt for Ni and Zn (Annex). However, the introduction of Cd ions into GGBS85 did not impact the precipitation of C-S-H. The formation of the Afm phase (C_4AH_{13}) can be detected for 0.1%wt of Cd, Cu and Ni (Fig. 2, (c)). The Monocarboaluminate phase was distinguished for 0.1%wt and 0.5%wt of Cd and Zn. The most

abundant ettringite precipitation was detected for 2%NiGGBS85 after 7 days of hydration compared to the other samples.

According to the XRD results of the Supersulfated formulation at 24 hours of storage, ettringite is the main hydration product of the control sample (Fig. 2, (d)). Ettringite was also detected for the lowest zinc nitrate dosage. At higher zinc amount the only phase identified on the graphs is gypsum. After 24 hours of hydration of SSC with copper addition, there was no ettringite precipitated. Regarding the results of the X-ray diffraction analysis of the Supersulfated formulation doped with nickel, there is almost even hydrates repartition and their intensity for the control sample SSC and 0.1%NiSSC, 0.5%NiSSC after 24 hours. With the addition of 2%$Ni(NO_3)_2$, the only detected phase was gypsum. With 2%wt of $Cd(NO_3)_2$ ettringite was detected after 24 h of storage but with lower intensity that for the other samples. An increase in the intensity of the ettringite peak was observed for 0.5%$Cd(NO_3)_2$ at 24h, this tendency was already reported in the study of Niu et al. [37] in the case of CSA cement mixed with $Cd(NO_3)_2$ where the intensities of diffraction peaks were higher in the samples with Cd compared to the sample without Cd. The general tendency of the impact of TM on the 24-hour evolution of the hydration products of SSC goes in the following order: Cu>Zn>Ni>Cd.

The absence of ettringite after 7 days of storage was observed for 0.5%wt and 2%wt of Zn and Cu as well as for 2%wt of Ni with gypsum as the major phase (Fig. 2, (e)). Nevertheless, all the samples with $Cd(NO_3)_2$ solution present a good uniform development of the hydration products at 7 days of storage. The effect of TM on the SSC hydration after 7 days of storage can be presented in the following order: Cu~Zn>Ni>Cd.

(a)

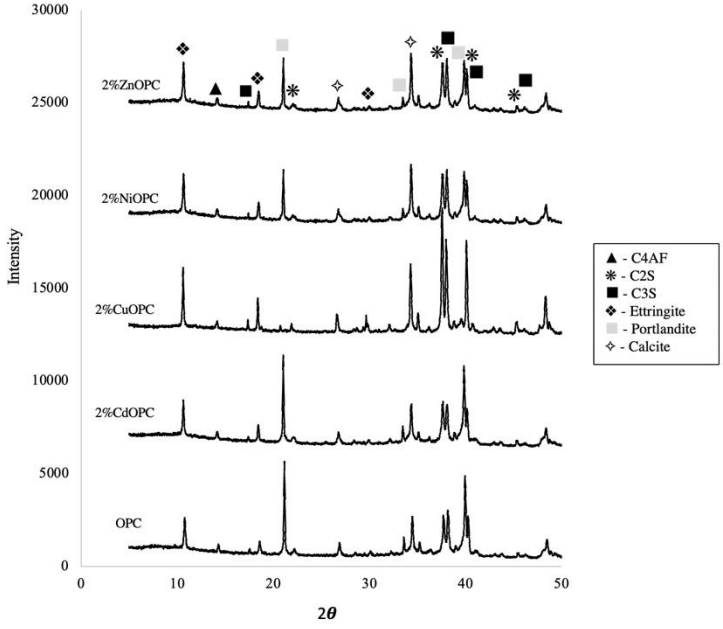
30000
25000
20000
15000
10000
5000
0
Intensity
2%ZnOPC
2%NiOPC
2%CuOPC
2%CdOPC
OPC
0
10
20
30
40
50
2θ
▲ - C4AF
✱ - C2S
■ - C3S
❖ - Ettringite
▩ - Portlandite
✧ - Calcite

379

(b)

(c)

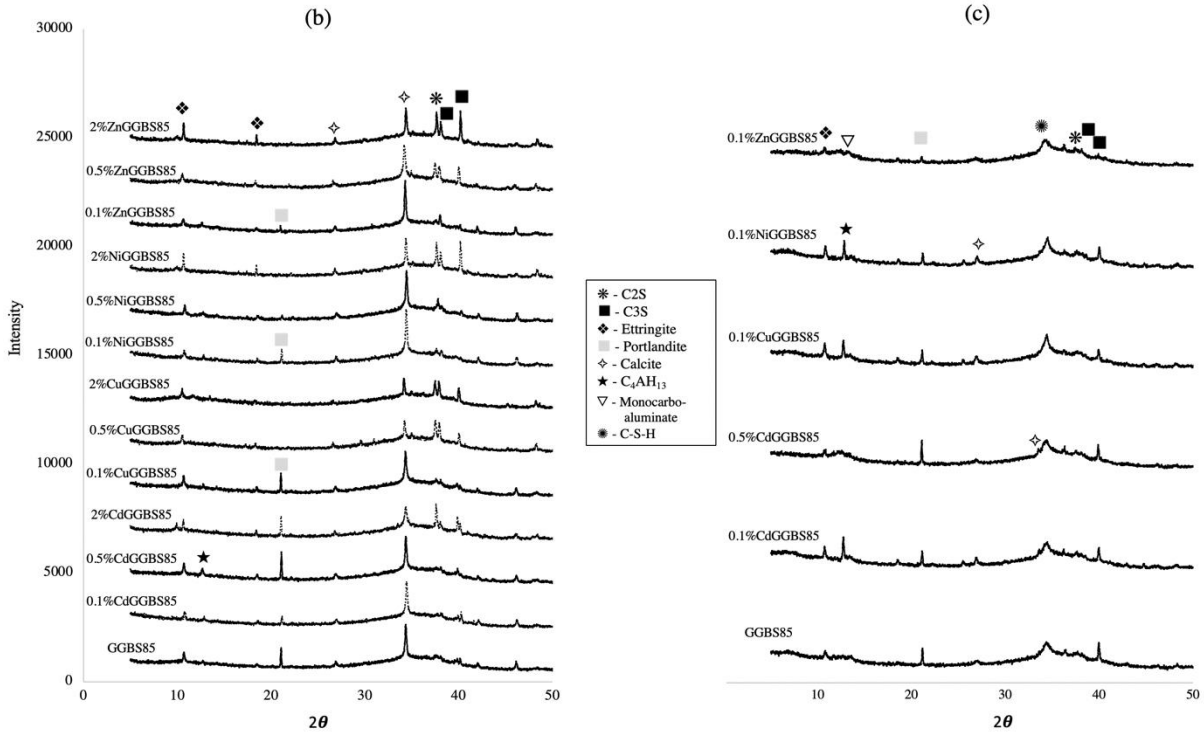
30000
25000
20000
15000
10000
5000
0
Intensity
2%ZnGGBS85
0.5%ZnGGBS85
0.1%ZnGGBS85
2%NiGGBS85
0.5%NiGGBS85
0.1%NiGGBS85
2%CuGGBS85
0.5%CuGGBS85
0.1%CuGGBS85
2%CdGGBS85
0.5%CdGGBS85
0.1%CdGGBS85
GGBS85
0
10
20
30
40
50
2θ
✱ - C2S
■ - C3S
❖ - Ettringite
▩ - Portlandite
✧ - Calcite
★ - C_4AH_{13}
▽ - Monocarbo-aluminate
✺ - C-S-H
0.1%ZnGGBS85
0.1%NiGGBS85
0.1%CuGGBS85
0.5%CdGGBS85
0.1%CdGGBS85
GGBS85
10
20
30
40
50
2θ

380

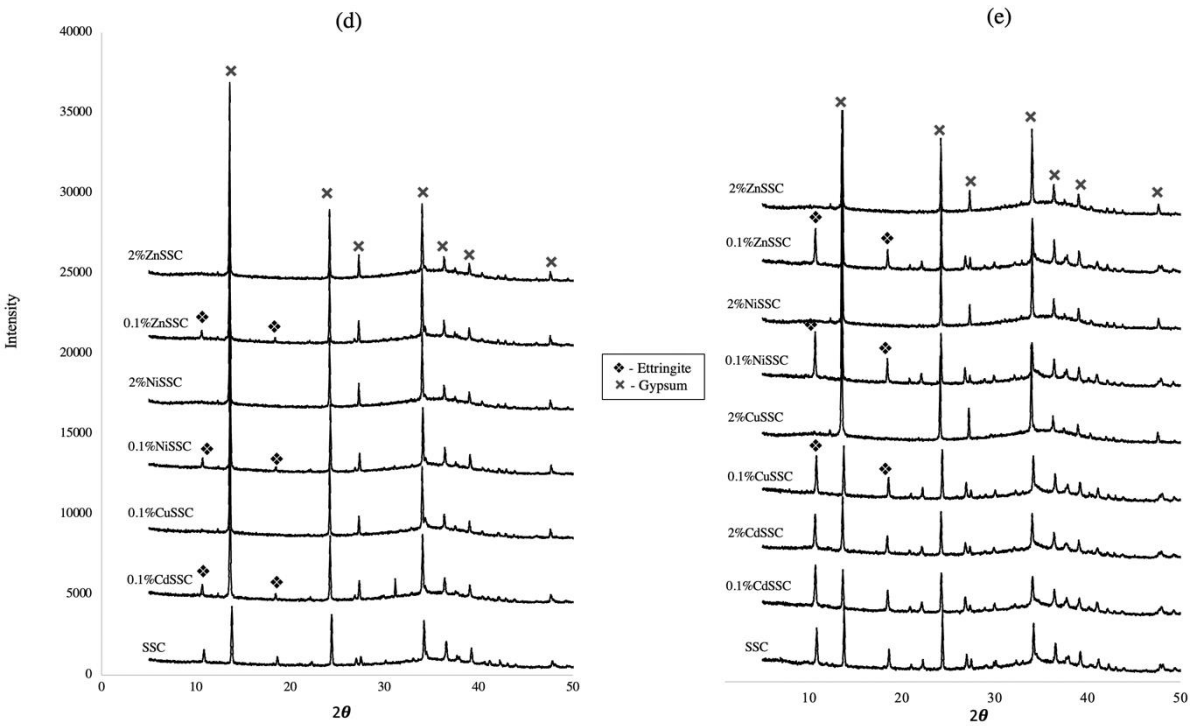

Fig. 2 XRD analysis of the OPC ((a) – 24 hours), GGBS85 ((b) – 24 hours, (c) – 7 days) and SSC ((d) – 24 hours, (e) – 7 days) formulations with the addition of Zn, Cu, Cd, Ni nitrate salts

4.3. Zeta Potential

The surface charge of the binders can be impacted by the size and type of an ion, as well as by the ionic strength of the solution [50]. Zeta potential measurements of both binders OPC and GGBS85 are presented in Fig. 3.

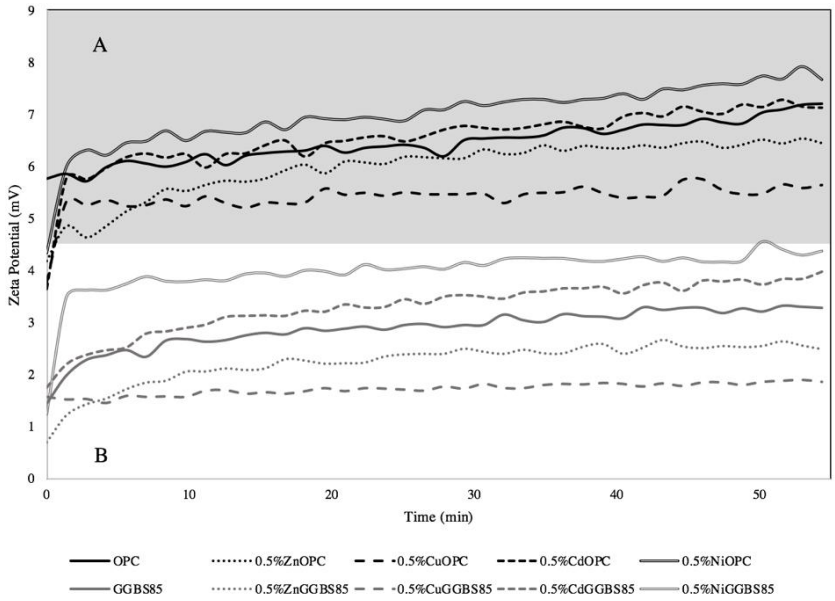

Fig. 3 Zeta Potential measurements of OPC (A) and GGBS85 (B) doped with 0,5%wt of Zn, Cu, Cd and Ni

Figure 3 (A) reveals the changes in the Zeta potential evolution of the 100%OPC binder mixed with four considered trace metals at 0.5%wt. The control sample reaches positive values from 6 to 8 mV over 60 min of the experiment. The positive value of the plain Portland cement arises from the increase in the concentration of calcium ions Ca^{2+} from Portland cement anhydrous minerals adsorbed on the negative surface of silanol groups during the hydration. The presence of trace metals shows a different effect on Zeta potential. A marked decrease in Zeta potential can be seen with zinc and copper salts – the first values for copper and OPC are around 3.5 mV and they increase to 5.6 mV over 60 min of hydration, whereas the OPC formulation in the presence of nickel ions shows a considerable increase in ζ potential. Positive values can be observed on the graph, from 4.3 mV it reaches almost 9 mV. However, the OPC binder in the cadmium salt solution exhibits almost the same ζ potential evolution as the control sample.

Zeta potential of the GGBS85 formulation in demineralized water and in four different trace metals nitrate solutions is set out in Fig. 3 (B). The values on the graph are noticeably lower than those of the OPC formulation, but are still positive. The changes in Zeta potential of the control sample when it was mixed with trace metals salts are fairly similar to the effect of the same considered trace metals on the plain OPC binder. The ζ potential values of the reference formulation GGBS85 were decreased

409 under the influence of zinc and especially copper nitrate ions. Unlike the effect of zinc and copper
410 nitrates, cadmium and nickel salts present a growth in ζ potential of the control sample. The samples
411 doped with nickel show an increase of ζ potential values from 1.24 mV to 4.4 mV and with cadmium
412 from 1.8 mV to 4 mV compared to the evolution of the reference formulation (from 1.4 mV to 3.3
413 mV) over all experiment time. The more negative charge of the surface in the presence of Cu and Zn
414 can be explained by the formation of neutral species with calcium or through interactions with surface
415 of cements grains involving the lower dissolution rate of the anhydrous phases. It highlights the
416 different impact of selected metals salts on the surface charge and therefore on hydration of the
417 binders. In addition to ζ potential, the lower conductivity values in Table 4 confirm the lower
418 dissolution rate for the Cu and Zn doped samples in contrast to Cd and Ni that accelerate the
419 dissolution through increasing surface deprotonation.
420

Formulation	**Conductivity** (mS/cm)	
	t=10 min	t=60 min
OPC	6.1	7.1
0.5%ZnOPC	5.3	6
0.5%CuOPC	5.3	5.6
0.5%NiOPC	6.2	7.3
0.5%CdOPC	6	6.9
GGBS85	2.7	3.3
0.5%ZnGGBS85	2.1	2.5
0.5%CuGGBS85	1.6	1.9
0.5%NiGGBS85	3.8	4.4
0.5%CdGGBS85	2.9	4

421 Table. 4 Conductivity measurements of OPC and GGBS85 doped with 0.5%wt of Zn, Cu, Cd and Ni
422 nitrate salts
423

424 4.4. ^{27}Al MAS NMR of OPC and GGBS85 in the presence of Zn and Cd
425
426 The ^{27}Al MAS NMR spectra of the hydrated Ordinary Portland cement mixed with trace metals salts
427 2%$Cd(NO_3)_2$ and 2%$Zn(NO_3)_2$ after 4 months of storage are presented in Fig. 4(a). The spectra are
428 composed of narrow well-defined signals in the Al^{VI} region and broad asymmetric signals in the Al^{IV}
429 range. OPC is known to give a signal with center of gravity at 86 ppm attributed to Al incorporated in
430 C_2S / tricalcium silicate C_3S and a second signal with center of gravity at 81 ppm corresponding to Al
431 in tricalcium aluminate C_3A; tetracalcium aluminoferrite phase being generally unobservable [51]. The

signal observed between 80 and 95 ppm could then be attributed to remaining Portland cement. Otherwise, the broad asymmetric peak ranging from 60 to 80 ppm should probably be attributed to the Al^{IV} incorporated in C-A-S-H phase resulting from the hydration of the OPC binder.

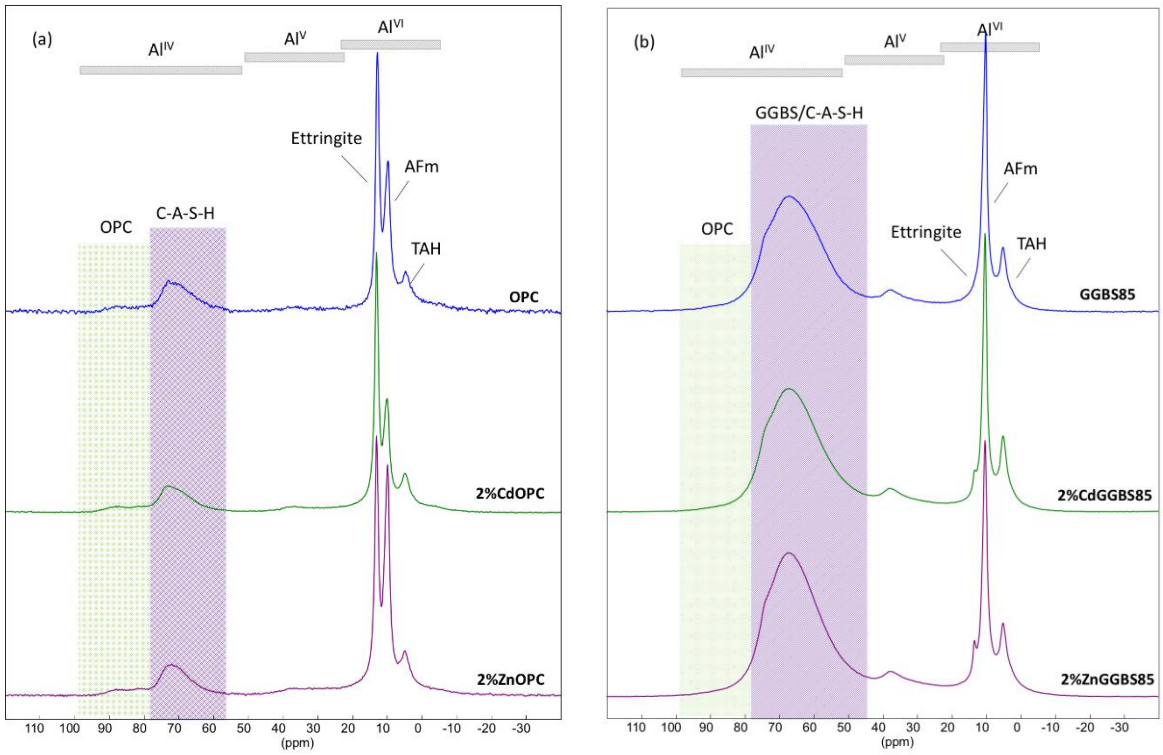

Fig. 4 ^{27}Al NMR spectra of (a) OPC, 2%ZnOPC, 2%CdOPC and (b) GGBS85, 2%ZnGGBS85, 2%CdGGBS85 after 4 months of hydration

In the range of 6-coordinated (octahedral) aluminium Al^{VI}, 3 sharp signals can be distinguished at 13, 10 and 4 ppm assigned respectively to aluminium in ettringite, AFm and third aluminate hydrate (TAH) [52]. This assignment shows that the three systems, pure or mixed with trace metals salts, are composed of the same aluminium containing phases. Moreover, if the relative amount of these phases slightly differ in one or the other case, the local environment of aluminium is the same. This seems to indicate that either trace metals are not incorporated in the hydrated phases resulting from OPC reaction, or their incorporation do not significantly change their structure as was shown by Pomiès et al. [53] in the case of cadmium.

Figure 4 (b) shows the ^{27}Al NMR spectra of the GGBS85 mix and of the mixtures 2%CdGGBS85 and 2%ZnGGBS85. As in the previous case, the spectra are composed of narrow signals in the Al^{VI}

450 domain unambiguously assigned to ettringite (13ppm), AFm (10ppm) and TAH (4.5 ppm). Ettringite
451 is absent in the case of GGBS85 formulation and weakly present on the spectra of 2%CdGGBS85 and
452 2%ZnGGBS85. However, the XRD analysis revealed the presence of ettringite in the GGBS85 system
453 at earlier age, therefore its transformation into the monosulfoaluminate (AFm) phase is suspected.
454 Thus, the ettringite crystals growth and the precipitation of cubic hydrated phases seem to increase
455 when some trace metals are added. This tendency was observed by Niu et al. [37] in the case of Cd
456 added into the CSA binder – the higher intensities of Ettringite diffraction were observed indicating
457 the enhanced nucleation and growth. Consequently, the presence of cadmium and zinc trace metals in
458 the GGBS85 system could enhance the formation of AFt and AFm.
459 In the Al^{IV} chemical shift range, no signal attributed to OPC can be detected. On the contrary, a broad
460 asymmetric signal is observed between 50 and 80 ppm corresponding to tetrahedral aluminium in the
461 highly depolymerised vitreous alumino-silicate network of GGBS. This asymmetric lineshape with a
462 steep high chemical shift edge and a trailing low chemical shift edge is characteristic of disordered
463 materials as glass [54]. Finally, a slight discontinuity can be observed at around 75 ppm which
464 revealed the formation of the C-A-S-H gel phase. According to the signal observed for C-A-S-H in the
465 case of pure OPC system (cf Fig. 4 (a)) another contribution should overlap with GGBS signal. The
466 addition of zinc or cadmium in the binder systems shows no significant difference for Al environment
467 inserted in the C-A-S-H.
468 The figure 5 shows the ^{29}Si MAS spectrum of OPC compared to MAS and $\{^1H\}$-^{29}Si CP-MAS spectra
469 of OPC mixed with 2%$Zn(NO_3)_2$ after 4 months of storage. The two MAS spectra are very similar and
470 composed of numerous Gaussian-like resonances spreading from -68 to -90 ppm. On the $\{^1H\}$-^{29}Si
471 CP-MAS spectrum only the signals relative to silicon in closed vicinity with proton are present, which
472 corresponds to edit specifically the signal assigned to C-A-S-H phase. This signal is relative to Q_1 and
473 Q_2 silicon species corresponding to the silicate chains of the C-A-S-H structure, partially substituted
474 by aluminium. The remaining MAS signal, between -68 and -76 ppm corresponds to the anhydrous
475 OPC. Considering the strong similarity of the MAS spectra of OPC and 2%ZnOPC, we can assume
476 that the addition of zinc in the binder systems shows no difference in the Si environment in the C-A-S-

H, either because the metal is not inserted in the structure, or the modifications are so weak that they are not detectable.

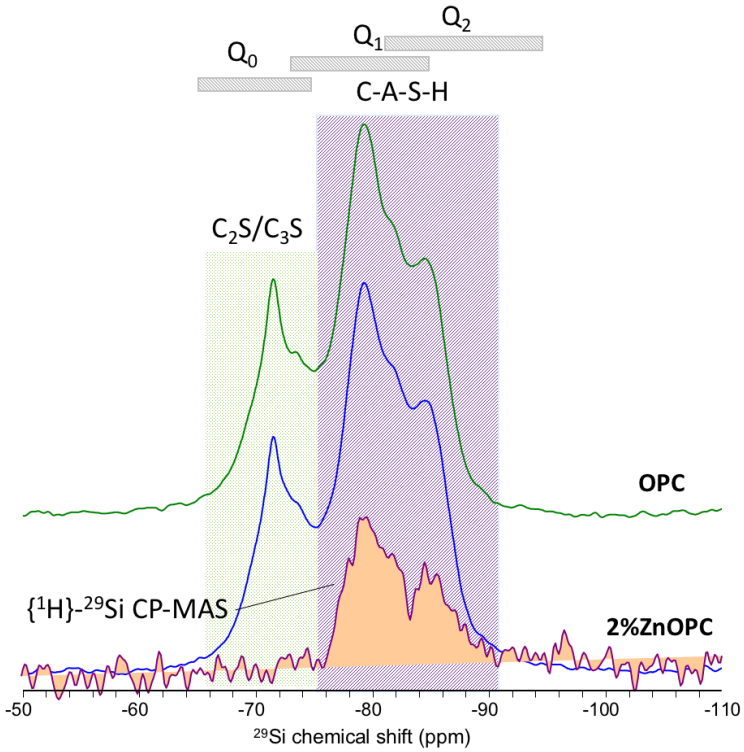

Fig. 5 ^{29}Si NMR spectra of OPC and 2%ZnOPC compared with {^{1}H}-^{29}Si NMR spectrum of 2%ZnOPC

4.5. XAFS. Species of Cadmium in OPC and SSC binders

K-edge XANES spectra of the OPC and Supersulfated formulations containing 0.5% of $CdCl_2$ are presented in Fig. 6 and are compared to the individual cadmium compounds. Cadmium is expected to be present solely in the (II) oxidation state in the studied binders. The presence of GGBS leads to the decrease in the amplitude of the XANES oscillations. The spectra differ from each other due to differences in coordination geometry and ligand forms of the absorber atom. The spectrum for 0.5%CdOPC is quite consistent with that of $Cd(OH)_2$ whereas the spectra for the SSC matrix is quite similar to that of CdS. Based on these first observations, it seems that the main species of cadmium is $Cd(OH)_2$ in the hydrated Portland cement and CdS in the hydrated matrix of high GGBS content. This difference of behaviour is partially related to the initial sulfurs content in the anhydrous compounds and the pH of the interstitial solution.

The type and the proportion of cadmium species in the cementitious matrix are determined by means of the EXAFS signal fingerprints of individual cadmium compounds based on the k²-weighted EXAFS functions (Fig. 7) (Eq. 1). The large content of CdS was also confirmed by the sample colour (yellowish brown) as observed by McWhinney and Cocke [49]. It results from the observations that cadmium reacts with sulfurs from GGBS. The added cadmium salt $CdCl_2$ is the second product present in the studied binders. In spite the care taken to avoid carbonation, $CdCO_3$ is the third compound for 0.5%CdOPC and 0.5%CdSSC. It is in agreement with [55] which found an increase in the surface carbonate formation in the metal-ion doped cement. This may be due to the presence of cations directly forming or indirectly inducing the formation of greater quantities of surface carbonate species.

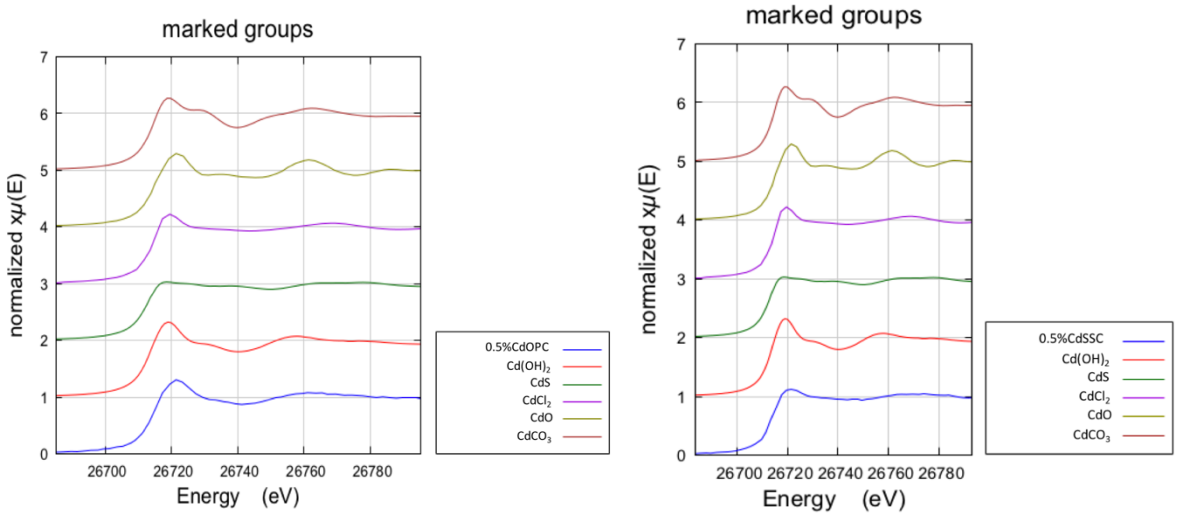

Fig. 6 K-edge XANES spectra of Cd in OPC binder (left) and in Supersulfated binder (right) compared to Cd individual compounds (colour should be used)

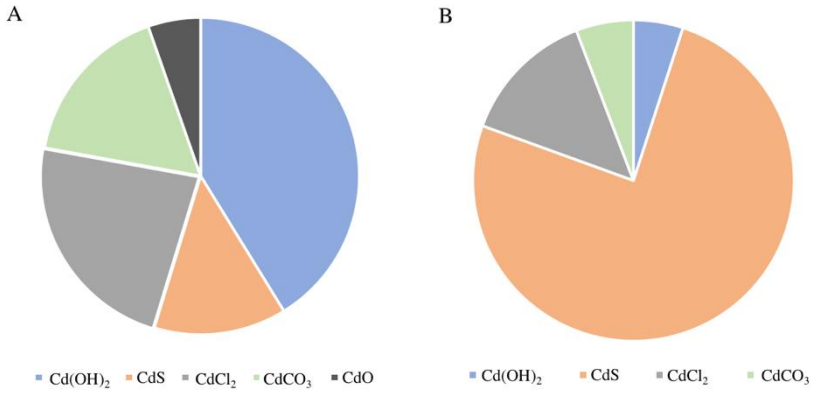

Fig. 7 Proportions of cadmium species in the OPC (A) and SSC (B) binder systems

5. Discussion

The results of the hydration heat evolution and XRD analysis indicate the retardation effect of zinc on the early hydration of the binders except for 0.1%ZnOPC. The retardation of hydration in the presence of zinc was attributed by many authors to the formation of the insoluble amorphous compound $CaZn_2(OH)_6.2H_2O$. The delay in cement hydration can be explained by the lack of calcium and hydroxides ions to saturate the solution in order to form $Ca(OH)_2$ and C-S-H gel due to the formation of calcium zincate $CaZn_2(OH)_6.2H_2O$ [19].

Indeed, [13] observed the stability of calcium zincate at early age of hydration with pH<12, that is why portlandite phase precipitates at a very low amount or does not precipitate. However, calcium zincate may dissolve at later ages of hydration (over 1 year) because of the hydration of C_3S at long term and pH raise to 12.5.

The lack of calcium ions due to the precipitation of complex salts species with Zn can explain lower ζ potential values for 0.5%ZnOPC and 0.5%GGBS85. The lower conductivity values of OPC and GGBS85 in the presence of zinc go in accordance with the extended induction period of 0.5%ZnOPC and 2%ZnOPC. The presence of zinc inhibits the C-S-H formation [56]. At the same time greater MHP values from the calorimetry measurements of 0.5%ZnOPC and 2%ZnOPC probably correspond to the changes in C-S-H morphology, in particular to the longer C-S-H needles formation [24]. [57] observed the enhanced outward growth of C-S-H at some dosages of zinc.

The evolution of the GGBS-based formulations seems to be attributed to the same mechanisms of the inhibition of hydration or even the absence of latter – the formation of calcium zincate, meaning the lack of the soluble calcium from C_2S and C_3S available for the formation of hydrates and for the pozzolanic reactions to be produced. In the case of GGBS85 this retardation effect is more pronounced than in the case of OPC because of the lower amount of available calcium. Therefore, the impact of the same content of zinc will retard greater the hydration of the GGBS-based samples as can be seen from the XRD and heat evolution results. The Supersulfated formulation contains only 1% of OPC needed for the activation of the system. Therefore, the effect of the presence of zinc is more important compared to OPC and GGBS85 arising from the fast sitting and the formation of gypsum.

Regarding the long term hydration of the OPC and GGBS-based binders in the presence of zinc, the ^{27}Al MAS NMR spectra showed no structural changes in the hydrates after 4 months of storage. It can be supposed that complexes formed with Zn exist as distinct particles or Zn is incorporated in the way that it does not modify the framework of the hydrates.

The addition of copper produced the most negative impact on the early hydration of the considered binders as observed in previous studies. Gineys et al. [21] reported a considerable delay effect of copper on the cement paste hydration with the compressive strength at 2 days tending to zero. This retardation effect from soluble copper salt at early age was attributed by the author to the low C_3S dissolution rate. Two possible models related to the retardation of hydration in presence of trace metals in cements' pastes were proposed:

- the first one explains the retardation effect by coating the surface of cements' grains by trace metals hydroxides

- the second one discusses the conversion of metal hydroxides species to metal hydroxyl. Due to this reaction there is a consumption of calcium and of hydroxides ions, and a lowering of pH, consequently the precipitation of $Ca(OH)_2$ and C-S-H are delayed and the dissolution of C_3S remains at low level. Chen et al. [13] detected the formation of the crystalline phase $Ca_2(OH)_4.4Cu(OH)_2{\cdot}H_2O$ in C3S suspension using XRD technique.

In our study, in the case of high dosage of copper addition, the Portland cement hydration was considerably impacted. The Zeta potential and conductivity measurements of OPC and GGBS85 in the presence of copper show the lowest values. The negative effect is more dramatic on the early hydration of the slag-based formulations than for the plane OPC sample due to the same mechanisms as described in the case of zinc addition - the deficiency of calcium ions due to the formation of complex Ca-Cu species.

In contrast to the copper and zinc impact, the addition of nickel nitrate produced mostly accelerating effect on the early hydration. Nickel at some specific dosages rather promotes the hydration of the cementitious materials by rapid dissolution of aluminium bearing phases and rapid precipitation of ettringite and minor Ni-LDH phases [58,59]. The acceleration of MHP was observed almost for all the samples as well as the more abundant ettringite formation. According to [60], nickel in the alkaline pH

568 range of 9-11 precipitates as $Ni(OH)_2$ and it remains as quite stable compound. It can be supposed that
569 the retardation of hydration of the GGBS-based formulations at 2%wt $Ni(NO_3)_2$ arises from the
570 $Ni(OH)_2$ precipitation and therefore the consumption of OH^-. The results of ζ potential demonstrate
571 the highest positive values for both OPC and GGBS-based formulations. It can be explained by the
572 simple hydroxides/Ni-LDH formation within the binders' alkaline solutions without disturbing the
573 availability of calcium for the formation of the main hydration products. The accelerated dissolution
574 can be confirmed by the highest conductivity values for OPC and GGBS85 in the presence of nickel
575 ions. The maximum conductivity values obtained for nickel suggests the higher and faster
576 supersaturation of solution. According to the results of [21] nickel did not affect the earlier
577 compressive strength of the cement samples after 2 days of storage compared to the negative impact of
578 zinc and copper.
579 Cadmium ions presented the less negative impact on the hydration of the binders in contrast to the
580 other considered trace metals as was observed via XRD, calorimetry and Zeta Potential experimental
581 techniques. The Cd introduction into considered binders accelerated the main hydration reactions for
582 OPC and GGBS85 and did not much affect the hydration of the SSC formulation. Data from several
583 studies suggests that cadmium in cement system will precipitate in form of cadmium hydroxide
584 following earlier hydration (pH>12.5), or cadmium carbonate (pH 9-11) [60,61]. The XANES spectra
585 confirm previous findings of formation of cadmium hydroxides as a major specie within the OPC
586 formulation. The acceleration effect of cadmium may be explained by the cadmium hydroxides
587 formation providing additional sites for the nucleation of C-S-H. Cartledge et al. [62] suggested the
588 physical inclusion of $Cd(OH)_2$ in C_2SH and the acceleration of C-S-H gel precipitation by the presence
589 of cadmium hydroxides. At the same time, the formation of a highly stable CdS was detected within
590 SSC formulation with an important prevalence of this cadmium compound due to the presence of
591 sulfurs in the slag.
592 It can thus be concluded that cadmium precipitates in form of simple hydroxides in the Portland
593 cement solution and in form of sulfurs within GGBS-based binders, it does not block the surface of the
594 anhydrous C_3S, C_2S, it does not interact with calcium ions necessary for hydrates formation. The long
595 term observations using the ^{27}Al MAS NMR spectra go in accordance with this assumption – the

incorporation of Cd did not modify the local environment of Al, it can be thus concluded that cadmium exists beyond the hydrates structure.

6. Conclusions

This work aimed to investigate the mechanisms responsible for the early hydration of GGBS-based binders in presence of different types of TM in S/S process. The study highlights that the early age hydration of the binders in presence of TM were not similarly affected, as it follows the order SSC>GGBS85>OPC. The trace metals ions impact the binding agent's early reactions depending on precipitated TM compounds. The results of the study can be categorized according to the effect of the considered trace metals on the hydration kinetic at early age:

1) Copper and zinc mostly retarded the hydration of OPC, GGBS85, SSC formulations. It can be concluded that zinc and copper precipitate in form of complex calcium hydroxides compounds such as calcium zincate $CaZn_2(OH)_6.2H_2O$ and $Ca_2(OH)_4.4Cu(OH)_2{\cdot}H_2O$. retard the hydration through the depletion of calcium ions. The extended induction period corresponds to the equilibrium of the system with low dissolution rate of the anhydrous phases of the binders. Once the trace metals are incorporated in complex calcium hydroxides, the nucleation of C-S-H may occur.
2) Nickel overall accelerated the hydration of binders. The acceleration of MHP was observed almost for all the samples as well as the more abundant ettringite formation. The formation of Ni-LDH can be expected to provide additional seeds for hydration. The results of ζ potential demonstrate the positive values that can be explained by the simple hydroxides/Ni-LDH formation without disturbing the availability of calcium for the formation of the main hydration products.
3) Cadmium accelerated the main hydration reactions for OPC and GGBS85 and did not much affect the hydration of the SSC formulation. In the OPC based formulations, $Cd(OH)_2$ is the main phase. The acceleration effect of cadmium may be explained by the cadmium hydroxides formation providing additional sites for the nucleation of C-S-H. Calcium ions remain available for the formation of the hydration products. This metal increased the surface charge inducing

higher dissolution rate of the minerals. At the same time, the formation of a highly stable CdS was detected within SSC formulation with an important prevalence of this cadmium compound due to the presence of sulfurs in the slag.

Consequently, the results from this paper confirm the complexity of the system 'GGBS-Binding agents-Trace metals' and demonstrate that metal cations may strongly impact the hydration kinetic by retarding/accelerating or completely annihilating the early hydration reactions but without modifying hydration products. The waste matrix must be well studied before the S/S treatment in order to ensure an optimized binder solution.

References

[1] C. Alzieu, Dragages et environnement marin, (1999) 225.
[2] OSPAR Convention, OSPAR Commission. (1998). https://www.ospar.org/ (accessed June 15, 2020).
[3] Z. Shen, F. Jin, D. O'Connor, D. Hou, Solidification/Stabilization for Soil Remediation: An Old Technology with New Vitality, Environ. Sci. Technol. 53 (2019) 11615–11617. https://doi.org/10.1021/acs.est.9b04990.
[4] B. Guo, B. Liu, J. Yang, S. Zhang, The mechanisms of heavy metal immobilization by cementitious material treatments and thermal treatments: A review, Journal of Environmental Management. 193 (2017) 410–422. https://doi.org/10.1016/j.jenvman.2017.02.026.
[5] S. Paria, P.K. Yuet, Solidification–stabilization of organic and inorganic contaminants using portland cement: a literature review, Environ. Rev. 14 (2006) 217–255. https://doi.org/10.1139/a06-004.
[6] Spence & Shi, Stabilization and Solidification of Hazardous, Radioactive, and Mixed Wastes, CRC Press. (2005). https://www.routledge.com/Stabilization-and-Solidification-of-Hazardous-Radioactive-and-Mixed-Wastes/Spence-Shi/p/book/9780367393410 (accessed June 15, 2020).
[7] Y. Yi, L. Gu, S. Liu, Microstructural and mechanical properties of marine soft clay stabilized by lime-activated ground granulated blastfurnace slag, Applied Clay Science. 103 (2015) 71–76. https://doi.org/10.1016/j.clay.2014.11.005.
[8] M.L. Allan, L.E. Kukacka, Blast furnace slag-modified grouts for in situ stabilization of chromium-contaminated soil, Waste Management. 15 (1995) 193–202. https://doi.org/10.1016/0956-053X(95)00017-T.
[9] J. Deja, Immobilization of Cr6+, Cd2+, Zn2+ and Pb2+ in alkali-activated slag binders, Cement and Concrete Research. 32 (2002) 1971–1979. https://doi.org/10.1016/S0008-8846(02)00904-3.
[10] R.B. Kogbara, A review of the mechanical and leaching performance of stabilized/solidified contaminated soils, Environ. Rev. 22 (2014) 66–86. https://doi.org/10.1139/er-2013-0004.
[11] L. Wang, K. Yu, J.-S. Li, D.C.W. Tsang, C.S. Poon, J.-C. Yoo, K. Baek, S. Ding, D. Hou, J.-G. Dai, Low-carbon and low-alkalinity stabilization/solidification of high-Pb contaminated soil, Chemical Engineering Journal. 351 (2018) 418–427. https://doi.org/10.1016/j.cej.2018.06.118.

[12] F. Jin, F. Wang, A. Al-Tabbaa, Three-year performance of in-situ solidified/stabilised soil using novel MgO-bearing binders, Chemosphere. 144 (2016) 681–688. https://doi.org/10.1016/j.chemosphere.2015.09.046.
[13] Q.Y. Chen, C.D. Hills, M. Tyrer, I. Slipper, H.G. Shen, A. Brough, Characterisation of products of tricalcium silicate hydration in the presence of heavy metals, Journal of Hazardous Materials. 147 (2007) 817–825. https://doi.org/10.1016/j.jhazmat.2007.01.136.
[14] J. Eggleton, K.V. Thomas, A review of factors affecting the release and bioavailability of contaminants during sediment disturbance events, Environment International. 30 (2004) 973–980. https://doi.org/10.1016/j.envint.2004.03.001.
[15] R. Malviya, R. Chaudhary, Factors affecting hazardous waste solidification/stabilization: A review, Journal of Hazardous Materials. 137 (2006) 267–276. https://doi.org/10.1016/j.jhazmat.2006.01.065.
[16] T. Zhang, J. Zou, Y. Li, Y. Jia, C.R. Cheeseman, Stabilization/Solidification of Strontium Using Magnesium Silicate Hydrate Cement, Processes. 8 (2020) 163. https://doi.org/10.3390/pr8020163.
[17] K.E. Clare, P.T. Sherwood, The effect of organic matter on the setting of soil-cement mixtures, J. Appl. Chem. 4 (2007) 625–630. https://doi.org/10.1002/jctb.5010041107.
[18] M. Mahedi, B. Cetin, A.Y. Dayioglu, Leaching behavior of aluminum, copper, iron and zinc from cement activated fly ash and slag stabilized soils, Waste Management. 95 (2019) 334–355. https://doi.org/10.1016/j.wasman.2019.06.018.
[19] Q.Y. Chen, M. Tyrer, C.D. Hills, X.M. Yang, P. Carey, Immobilisation of heavy metal in cement-based solidification/stabilisation: A review, Waste Management. 29 (2009) 390–403. https://doi.org/10.1016/j.wasman.2008.01.019.
[20] I. Fernández Olmo, E. Chacon, A. Irabien, Influence of lead, zinc, iron (III) and chromium (III) oxides on the setting time and strength development of Portland cement, Cement and Concrete Research. 31 (2001) 1213–1219. https://doi.org/10.1016/S0008-8846(01)00545-2.
[21] N. Gineys, G. Aouad, D. Damidot, Managing trace elements in Portland cement – Part I: Interactions between cement paste and heavy metals added during mixing as soluble salts, Cement and Concrete Composites. 32 (2010) 563–570. https://doi.org/10.1016/j.cemconcomp.2010.06.002.
[22] L. Lu, C. Xiang, Y. He, F. Wang, S. Hu, Early hydration of C3S in the presence of Cd2+, Pb2+ and Cr3+ and the immobilization of heavy metals in pastes, Construction and Building Materials. 152 (2017) 923–932. https://doi.org/10.1016/j.conbuildmat.2017.07.026.
[23] L. Aljerf, Effect of Thermal-cured Hydraulic Cement Admixtures on the Mechanical Properties of Concrete, Interceram - International Ceramic Review. (2015). https://doi.org/10.1007/BF03401142.
[24] K. Scrivener, A. Ouzia, P. Juilland, A. Kunhi Mohamed, Advances in understanding cement hydration mechanisms, Cement and Concrete Research. 124 (2019) 105823. https://doi.org/10.1016/j.cemconres.2019.105823.
[25] C. Weeks, R.J. Hand, J.H. Sharp, Retardation of cement hydration caused by heavy metals present in ISF slag used as aggregate, Cement and Concrete Composites. 30 (2008) 970–978. https://doi.org/10.1016/j.cemconcomp.2008.07.005.
[26] R. Cook, H. Ma, A. Kumar, Mechanism of tricalcium silicate hydration in the presence of polycarboxylate polymers, SN Appl. Sci. 1 (2019) 145. https://doi.org/10.1007/s42452-018-0153-1.
[27] P. Juilland, E. Gallucci, R. Flatt, K. Scrivener, Dissolution Theory Applied to the Induction Period in Alite Hydration, Cement and Concrete Research. 40 (2010) 831–844. https://doi.org/10.1016/j.cemconres.2010.01.012.
[28] A.M. Ley-Hernandez, J. Lapeyre, R. Cook, A. Kumar, D. Feys, Elucidating the Effect

716 of Water-To-Cement Ratio on the Hydration Mechanisms of Cement, ACS Omega. 3 (2018)
717 5092–5105. https://doi.org/10.1021/acsomega.8b00097.
718 [29] A. Bazzoni, Study of early hydration mechanisms of cement by means of electron
719 microscopy, in: 2014. https://doi.org/10.5075/epfl-thesis-6296.
720 [30] P. Aïtcin and R. Flatt, Science and Technology of Concrete Admixtures, Elsevier,
721 2016. https://doi.org/10.1016/C2015-0-00150-2.
722 [31] E. John, T. Matschei, D. Stephan, Nucleation seeding with calcium silicate hydrate –
723 A review, Cement and Concrete Research. 113 (2018) 74–85.
724 https://doi.org/10.1016/j.cemconres.2018.07.003.
725 [32] L. Nicoleau, E. Schreiner, A. Nonat, Ion-specific effects influencing the dissolution of
726 tricalcium silicate, Cement and Concrete Research. 59 (2014) 118–138.
727 https://doi.org/10.1016/j.cemconres.2014.02.006.
728 [33] H. Viallis-Terrisse, A. Nonat, J.-C. Petit, Zeta-Potential Study of Calcium Silicate
729 Hydrates Interacting with Alkaline Cations, Journal of Colloid and Interface Science. 244
730 (2001) 58–65. https://doi.org/10.1006/jcis.2001.7897.
731 [34] E.E. Hekal, E.A. Kishar, M.R. Mohamed, M.K. Mahmoud, B.A. Mohamed,
732 Inertization of lead by using blended cement pastes, HBRC Journal. 8 (2012) 153–158.
733 https://doi.org/10.1016/j.hbrcj.2012.10.001.
734 [35] H.N. Yoon, J. Seo, S. Kim, H.K. Lee, S. Park, Characterization of blast furnace slag-
735 blended Portland cement for immobilization of Co, Cement and Concrete Research. 134
736 (2020) 106089. https://doi.org/10.1016/j.cemconres.2020.106089.
737 [36] N. Garg, C.E. White, Mechanism of zinc oxide retardation in alkali-activated
738 materials: an in situ X-ray pair distribution function investigation, J. Mater. Chem. A. 5
739 (2017) 11794–11804. https://doi.org/10.1039/C7TA00412E.
740 [37] M. Niu, Comparative study of immobilization and mechanical properties of
741 sulfoaluminate cement and ordinary Portland cement with different heavy metals,
742 Construction and Building Materials. (2018) 12.
743 [38] M. Keppert, B. Doušová, P. Reiterman, S. Kolouskova, M. Záleská, R. Černý,
744 Application of heavy metals sorbent as reactive component in cementitious composites,
745 Journal of Cleaner Production. 199 (2018). https://doi.org/10.1016/j.jclepro.2018.07.198.
746 [39] B. Li, S. Zhang, Q. Li, N. Li, B. Yuan, W. Chen, H.J.H. Brouwers, Q. Yu, Uptake of
747 heavy metal ions in layered double hydroxides and applications in cementitious materials:
748 Experimental evidence and first-principle study, Construction and Building Materials. 222
749 (2019) 96–107. https://doi.org/10.1016/j.conbuildmat.2019.06.135.
750 [40] T. Gutsalenko, M. Chaouche, P. Seymour, L. Frouin, Effects of GGBS on the
751 solidification/stabilization of port sediments contaminatedwith heavy metals, (2018) 6.
752 [41] C. Gervais, S.K. Ouki, Performance study of cementitious systems containing zeolite
753 and silica fume: effects of four metal nitrates on the setting time, strength and leaching
754 characteristics, (2002) 14.
755 [42] A. Duran, R. Sirera, M. Pérez-Nicolás, I. Navarro-Blasco, J.M. Fernández, J.I.
756 Alvarez, Study of the early hydration of calcium aluminates in the presence of different
757 metallic salts, Cement and Concrete Research. 81 (2016) 1–15.
758 https://doi.org/10.1016/j.cemconres.2015.11.013.
759 [43] EN 15167-1:2006 - Ground granulated blast furnace slag for use in concrete, mortar
760 and grout - Part 1: Definitions, specifications and conformity criteria, ITeh Standards Store.
761 (n.d.). https://standards.iteh.ai/catalog/standards/cen/ff51b993-7c12-42cf-a561-
762 ddafacccc108/en-15167-1-2006 (accessed June 2, 2021).
763 [44] A. Yoneyama, H. Choi, M. Inoue, J. Kim, M. Lim, Y. Sudoh, Effect of a
764 Nitrite/Nitrate-Based Accelerator on the Strength Development and Hydrate Formation in
765 Cold-Weather Cementitious Materials, (2021) 14.

766 [45] L. Matejka, P. Siler, R. Novotny, J. Svec, J. Masilko, F. Soukal, Negative effect of
767 zinc compounds on hydration kinetics of ordinary Portland cement, IOP Conf. Ser.: Mater.
768 Sci. Eng. 1039 (2021) 012004. https://doi.org/10.1088/1757-899X/1039/1/012004.
769 [46] J. Markus, A.B. McBratney, A review of the contamination of soil with lead: II.
770 Spatial distribution and risk assessment of soil lead, Environment International. 27 (2001)
771 399–411. https://doi.org/10.1016/S0160-4120(01)00049-6.
772 [47] G.E. Voglar, D. Lestan, Solidification/stabilisation of metals contaminated industrial
773 soil from former Zn smelter in Celje, Slovenia, using cement as a hydraulic binder, J. Hazard.
774 Mater. 178 (2010) 926–933. https://doi.org/10.1016/j.jhazmat.2010.02.026.
775 [48] D. Massiot, F. Fayon, M. Capron, I. King, S. Cal, B. Alonso, J.-O. Durand, B. Bujoli,
776 Z. Gan, G. Hoatson, Modelling One- and Two-dimensional Solid-State NMR Spectra,
777 Magnetic Resonance in Chemistry. 40 (2002) 70–76. https://doi.org/10.1002/mrc.984.
778 [49] H.G. McWhinney, D.L. Cocke, A surface study of the chemistry of zinc, cadmium,
779 and mercury in portland cement, Waste Management. 13 (1993) 117–123.
780 https://doi.org/10.1016/0956-053X(93)90003-F.
781 [50] Y. Yukselen-Aksoy, A. Kaya, The Zeta Potential of a Mixed Mineral Clay in the
782 Presence of Cations, 1 (2016) 8.
783 [51] J. Skibsted, E. Henderson, H.J. Jakobsen, Characterization of calcium aluminate
784 phases in cements by aluminum-27 MAS NMR spectroscopy, Inorg. Chem. 32 (1993) 1013–
785 1027. https://doi.org/10.1021/ic00058a043.
786 [52] M.D. Andersen, H.J. Jakobsen, J. Skibsted, A new aluminium-hydrate species in
787 hydrated Portland cements characterized by 27Al and 29Si MAS NMR spectroscopy, Cement
788 and Concrete Research. 36 (2006) 3–17. https://doi.org/10.1016/j.cemconres.2005.04.010.
789 [53] M.-P. Pomiès, N. Lequeux, P. Boch, Speciation of cadmium in cement Part I. Cd2+
790 uptake by C-S-H, Cement and Concrete Research. (2001) 7.
791 [54] D. Neuville, L. Cormier, V. Montouillout, P. Florian, F. Millot, J.-C. Rifflet, D.
792 Massiot, Structure of Mg- and Mg/Ca Aluminosilicate Glasses: 27Al NMR and Raman
793 Spectroscopy Investigations, American Mineralogist - AMER MINERAL. 93 (2008) 1721–
794 1731. https://doi.org/10.2138/am.2008.2867.
795 [55] H.G. Mcwhinney, D.L. Cocke, Original Contribution a Surface Study of the
796 Chemistry of Zinc , Cadmium , and Mercury in Portland Cement, 13 (1993) 117–123.
797 [56] A. Stumm, K. Garbev, G. Beuchle, L. Black, P. Stemmermann, R. Nüesch,
798 Incorporation of zinc into calcium silicate hydrates, Part I: formation of C-S-H(I) with
799 C/S=2/3 and its isochemical counterpart gyrolite, Cement and Concrete Research. 35 (2005)
800 1665–1675. https://doi.org/10.1016/j.cemconres.2004.11.007.
801 [57] A. Bazzoni, S. Ma, Q. Wang, X. Shen, M. Cantoni, K.L. Scrivener, The Effect of
802 Magnesium and Zinc Ions on the Hydration Kinetics of C3S, J. Am. Ceram. Soc. 97 (2014)
803 3684–3693. https://doi.org/10.1111/jace.13156.
804 [58] A.M. Scheidegger, E. Wieland, A.C. Scheinost, R. Dähn, P. Spieler, Spectroscopic
805 Evidence for the Formation of Layered Ni−Al Double Hydroxides in Cement, Environ. Sci.
806 Technol. 34 (2000) 4545–4548. https://doi.org/10.1021/es0000798.
807 [59] M. Vespa, R. Dähn, D. Grolimund, E. Wieland, A.M. Scheidegger, Spectroscopic
808 Investigation of Ni Speciation in Hardened Cement Paste, Environ. Sci. Technol. 40 (2006)
809 2275–2282. https://doi.org/10.1021/es052240q.
810 [60] M. Achternbosch, K.R. Bräutigam, N. Hartlieb, C. Kupsch, U. Richers, P.
811 Stemmermann, M. Gleis, Heavy metals in cement and concrete resulting from the co-
812 incineration of wastes in cement kilns with regard to the legitimacy of waste utilisation,
813 (2003). https://doi.org/10.5445/IR/270055717.
814 [61] C.E. Halim, R. Amal, D. Beydoun, J.A. Scott, G. Low, Implications of the structure of
815 cementitious wastes containing Pb(II), Cd(II), As(V), and Cr(VI) on the leaching of metals,

816 Cement and Concrete Research. 34 (2004) 1093–1102.
817 https://doi.org/10.1016/j.cemconres.2003.11.025.
818 [62] F.K. Cartledge, L.G. Butler, D. Chalasani, H.C. Eaton, F.P. Frey, E. Herrera, M.E.
819 Tittlebaum, S.L. Yang, Immobilization mechanisms in solidifiction/stabilization of cadmium
820 and lead salts using portland cement fixing agents, Environ. Sci. Technol. 24 (1990) 867–873.
821 https://doi.org/10.1021/es00076a012.
822